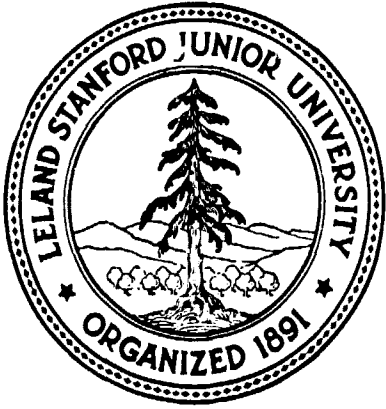


General Disclaimer

One or more of the Following Statements may affect this Document

- This document has been reproduced from the best copy furnished by the organizational source. It is being released in the interest of making available as much information as possible.
- This document may contain data, which exceeds the sheet parameters. It was furnished in this condition by the organizational source and is the best copy available.
- This document may contain tone-on-tone or color graphs, charts and/or pictures, which have been reproduced in black and white.
- This document is paginated as submitted by the original source.
- Portions of this document are not fully legible due to the historical nature of some of the material. However, it is the best reproduction available from the original submission.



Progress Report No. 5

MECHANISM OF THE PHOTOVOLTAIC EFFECT IN II-VI COMPOUNDS

National Aeronautics and Space Administration
Lewis Research Center
Cleveland, Ohio

April 1 - June 30, 1969

School of Engineering
Department of Materials Science
Stanford University
Stanford, California

Grant NGR-05-020-214 S-1

Principal Investigator
Richard H. Bube, Professor

Report Prepared By:

R.H. Bube
P.F. Lindquist

N69-38072

(ACCESSION NUMBER)

30

(PAGES)

(THRU)

1

(CODE)

26

(CATEGORY)

SU-DMS-69-R-67

(NASA CR OR TMX OR AD NUMBER)

CR# 105971

Department of MATERIALS SCIENCE
STANFORD UNIVERSITY

Progress Report No. 5

MECHANISM OF THE PHOTOVOLTAIC EFFECT IN II-VI COMPOUNDS

National Aeronautics and Space Administration
Lewis Research Center
Cleveland, Ohio

April 1 - June 30, 1969

School of Engineering
Department of Materials Science
Stanford University
Stanford, California

Grant NGR-05-320-214 S-1

Principal Investigator
Richard H. Bube, Professor

Report Prepared By:

R.H.Bube
P.F.Lindquist

SU-DMS-69-R-67

CONTENTS

SUMMARY	
I. INTRODUCTION	1
II. EXPERIMENTAL PROCEDURE	
A. Sample Preparation	1
B. Measurements	2
III. RESULTS	
A. Room Temperature Measurements	
1. General Results	2
2. I-V Characteristics	4
3. C-V Curves	5
4. Spectral Response	5
5. Time-Dependent Reverse Current in the Light	6
6. Pulsed Forward I-V Characteristics	6
B. Low-Temperature Measurements	7
IV. DISCUSSION	8
V. CONCLUSIONS	9
REFERENCES	11

SUMMARY

A systematic study of non-heat-treated single-crystal Cu_2S -CdS heterojunctions has been initiated. In particular, the effects of Cu_2S layer thickness and of CdS crystallographic orientation (A vs. B face) have been investigated. The basic mechanism of charge transport across the junction is a tunneling process, presumably through a conduction band spike. Major differences between A- and B-face behavior are found in the measurements of (1) growth rate of the Cu_2S layer, (2) open-circuit voltage, (3) dependence of the slope of the C-V curve on layer thickness. The short-circuit current density decreases with increasing layer thickness for both A- and B-face samples, with A-face samples having the higher current density for thin layers. A possible interpretation of certain features of these data may be found in terms of a piezoelectric effect and of interface states.

I. INTRODUCTION

A systematic study of the properties of Cu_2S -CdS heterojunctions has been conducted with the following principal fabrication variables: dipping time, crystallographic orientation of the CdS, and surface condition before dipping. The purpose of this investigation was to clarify the dependence of the properties of the Cu_2S -CdS heterojunction on properties of the interface. All measurements were carried out on non-heat-treated cells in order to avoid possible complications due to the phase transition in Cu_2S at about 105°C .

II. EXPERIMENTAL PROCEDURE

A. Sample Preparation

Rectangular bars were cut from conducting (1 ohm-cm) "pure" CdS single crystals grown by sublimation in a moving temperature gradient.¹ The bars were approximately 1 mm x 4 mm in area and 0.5-1 mm thick, and were cut with the large faces normal to the c-axis within 5° . The A face (Cd-rich) and the B face (S-rich) were distinguished by etching in concentrated HCl. The two large faces of each crystal bar were mechanically polished with α -alumina on silk. Ohmic indium contacts were attached to both ends of each crystal bar on the face opposite the one subsequently dipped. The face to be dipped was either left in the as-polished condition or etched for two minutes in a solution of KMnO_4 in H_2SO_4 .

The Cu_2S layer was formed by dipping the crystals in a saturated solution of CuCl in water, to which KCl and hydroxylamine hydrochloride were added. The KCl increases the concentration of cuprous ion complexes in solution, and the hydroxylamine hydrochloride prevents the copper from oxidizing to the cupric (+2) state. HCl was also added to the solution to give a starting pH of about 3. The solution was blanketed with argon and

sealed after immersion of the samples. The reaction occurred on only one face of each crystal bar, the other faces being masked by black wax. The solution was prepared in the same manner each time. The dipping temperature was 75°C , controlled to better than 1°C during most of the dipping time. The samples prepared thus far by this procedure are listed in Table I.

B. Measurements

The following measurements have been made at 300°K on all samples except the last two in Table I:

1. Spectral response of i_{sc} and V_{oc} , 5000-14,000Å, backwall,
2. Dark and light I-V characteristic on diode curve tracer,
3. Capacitance-voltage (C-V), dark and white light, 1 MHz,
4. I_{sc} and V_{oc} vs. light intensity (white light),
5. I-V characteristic in dark, point-by-point, forward and reverse,
6. Time-dependent reverse current in light,
7. Pulsed forward I-V characteristic in dark.

In addition, low temperature measurements ($100^{\circ} - 300^{\circ}\text{K}$) are now in progress. Only several selected samples have been measured to date. The measurements being made are:

8. I-V characteristic in dark, point-by-point, forward and reverse, vs. T,
9. V_{oc} and I_{sc} (white light) vs. T,
10. C-V, dark and white light, 1 MHz, vs. T.

III. RESULTS

A. Room Temperature Measurements

1. General Results

Data for 10 samples measured at room temperature are presented in Table II. Values of I_{sc} and V_{oc} were obtained in white light of integrated intensity of 280 mw/cm^2 from a tungsten source. The values of capacitance and conductance per unit area, C/A and G/A, were measured with a Boonton Model 75-D

TABLE I

Summary of Single-Crystal Samples Dipped at 75°C

<u>Dipping Time, hr</u>	<u>Dipped Face</u>	<u>Surface Condition</u>
2	A	P *
2	A	P + E **
2	B	P
2	B	P + E
4	A	P
4	A	P + E
8	A	P
8	A	P + E
8	B	P
8	B	P + E
18	B	P
18	B	P + E

* P - polished only

** P + E - polished and etched

TABLE II

Tabulation of Room Temperature Data for 10 Single Crystal Cells

Sample	Cu ₂ S Thickness, μ	J_{sc} , ma/cm ²	V_{oc} , mv	(C/A), 10 ⁴ pf/cm ² (G/A), 10 ⁵ μ U/cm ²	J_0 , 10 ⁻⁸ amp/cm ²	ϕ , Volts		
						I-V	C-V	
2-A(P)	35	6.73	450	5.36	2.00	9.6	0.6	0.8
2-A(P+E)	35	6.20	455	5.37	1.70	6.9	0.9	0.9
2-B(P)	<10	5.58	470	4.67	1.38	2.8	0.7	1.0
2-B(P+E)	<10	6.18	475	4.98	1.01	0.15	0.7	0.9
4-A(P)	93	4.00	420	7.57	2.39	3.0	-	-
4-A(P+E)	108	4.45	400	6.32	2.46	31	-	-
8-A(P)	199	3.62	400	11.46	1.82	8.2	0.65	0.62
8-A(P+E)	210	3.15	400	11.39	1.64	9.2	0.65	0.65
8-B(P)	68	5.45	455	4.73	0.49	3.8	0.8	0.8
8-B(P+E)	69	4.35	465	4.10	0.40	3.2	0.7	0.8

Capacitance Bridge operating at 1 MHz with a signal amplitude of about 20 mv peak-to-peak. The values of the "saturation current" J_0 were obtained by extrapolating the forward dark I-V characteristics to zero voltage. The "forward barrier" voltage ϕ was obtained by (a) extending the forward dark I-V characteristic into the series-resistance limited regime and extrapolating to zero current, and (b) plotting C^{-n} vs. V and extrapolating to $C^{-n} = 0$. The exponent n is derived from a plot of $\log C$ vs. $\log (\phi - V)$ in which ϕ is estimated by another technique, such as (a).

An examination of Table II shows a large difference in growth rate of the Cu_2S between the A (Cd, 0001) face and the B (S, 000 $\bar{1}$) faces. These data are plotted in Figure 1. Another interesting feature is the fact that the slope is somewhat greater than unity, which indicates that the rate control is not by a simple diffusion process. This is in apparent contradiction to the results reported by Singer and Faeth², who showed a linear relation between the weight gain and $t^{1/2}$ as would be expected for a diffusion-controlled process. A possible explanation is that these investigators apparently allowed the reaction to proceed on all faces of their crystals simultaneously; the existence of large variations in growth rate for different crystallographic directions might average out in an overall rate law of $t^{1/2}$.

Table II also indicates that the open-circuit voltage for B-face samples is consistently higher than for A-face samples, whereas the relative values of short-circuit current seem to depend primarily on layer thickness. For example, the A-face samples have higher J_{sc} than B-face samples for the 2-hour dipping, but the situation is reversed for the 8-hour dipping.

Another interesting feature is that the zero-bias capacitance per unit area increases markedly with increasing dipping time (layer thickness) for

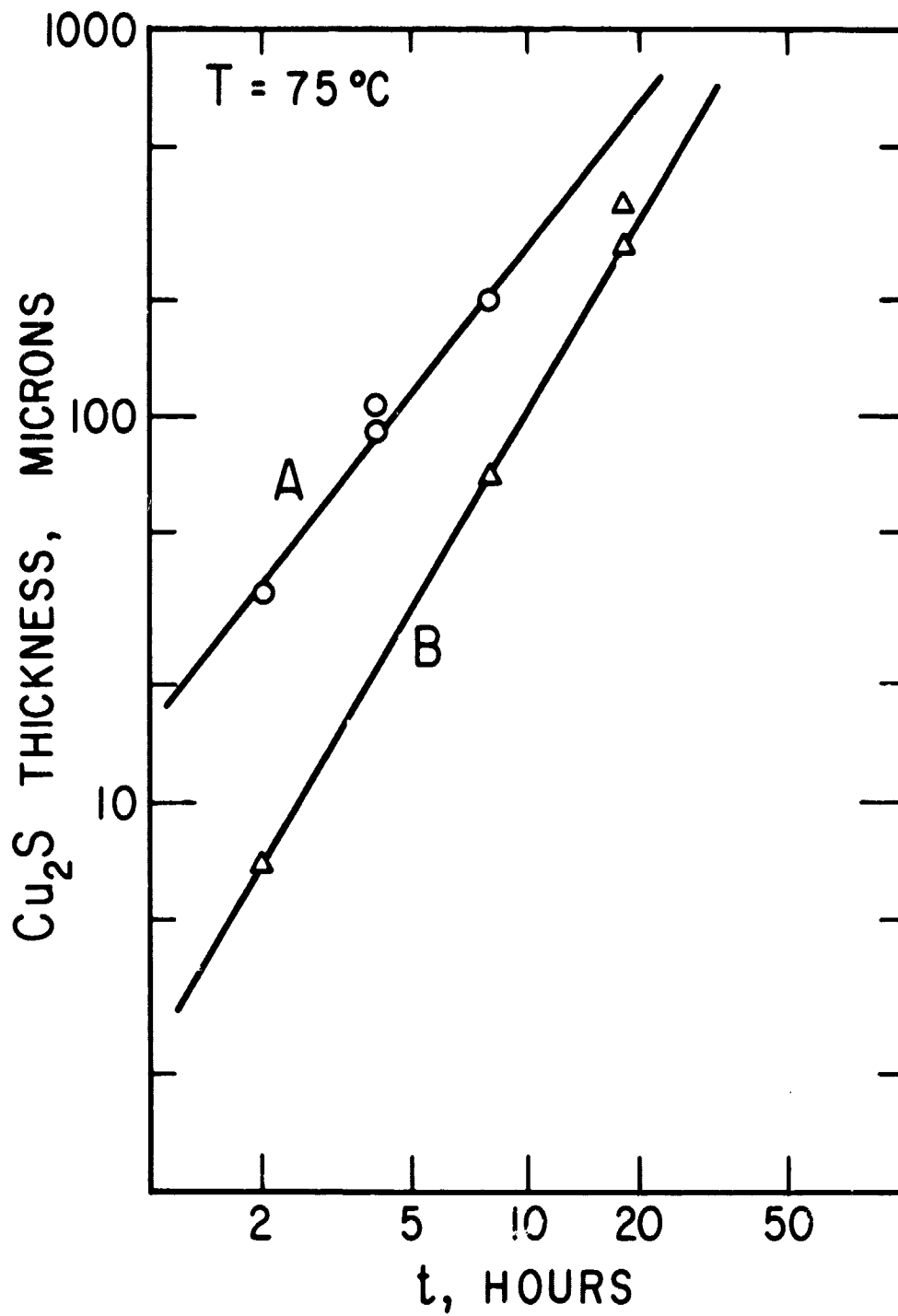


Fig. 1 - Thickness of Cu₂S vs. Time of Dipping at 75°C, for "A" and "B" Faces of CdS

the A-face samples, but remains essentially constant and perhaps even decreases slightly with increasing layer thickness for the B-face samples.

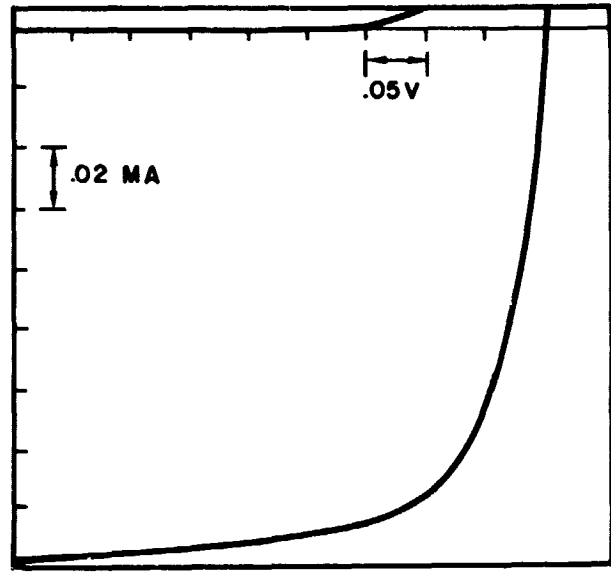
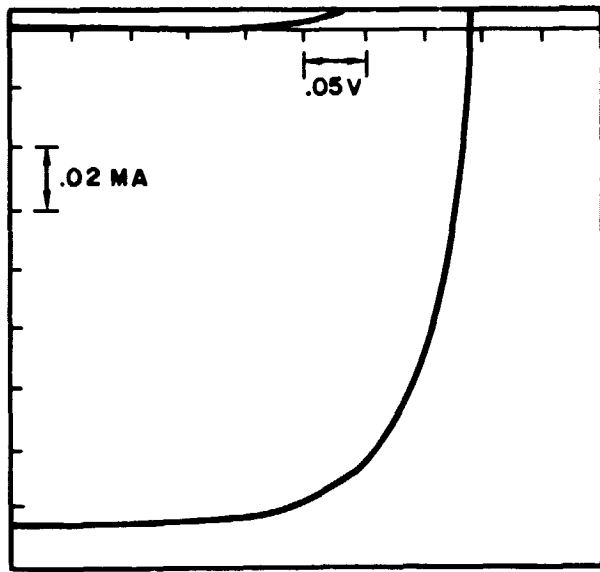
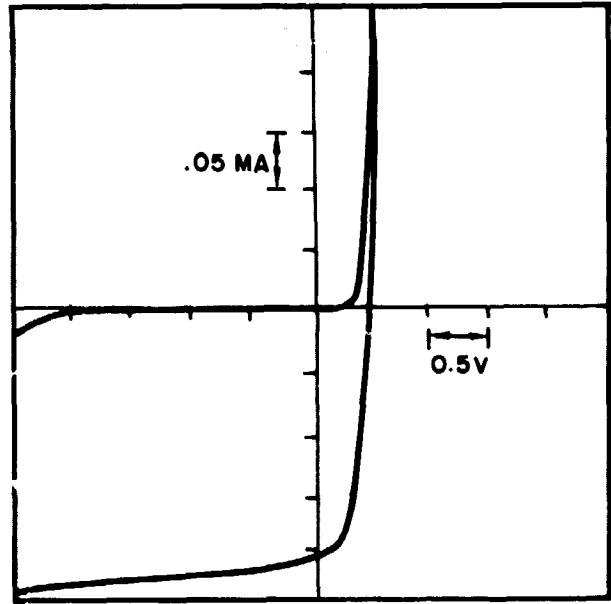
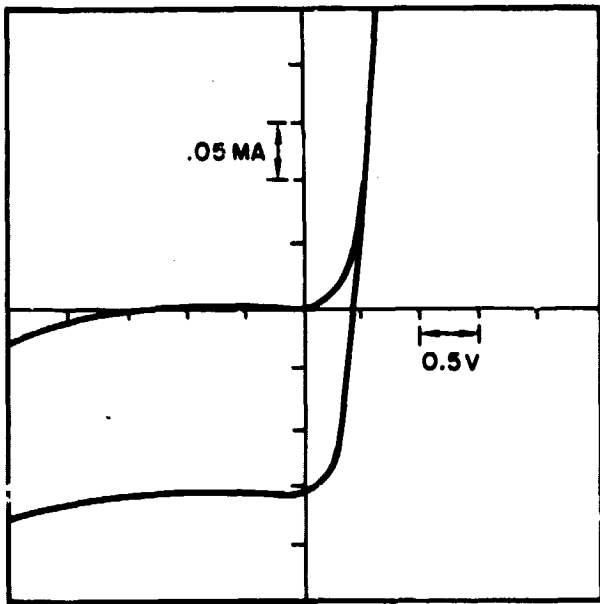
No consistent variation in J_0 is apparent from Table II. The values fall mainly in the range of 10^{-8} to 10^{-7} amp/cm².

Reasonable agreement is found in the values of ϕ , the "forward barrier voltage", as determined by capacitance data and by pulsed forward I-V characteristics. In six out of eight cases where a comparison is possible, the value of ϕ is slightly larger for the B-face samples.

2. I-V Characteristics

Figure 2 shows the dark and light I-V characteristics for two cells as displayed on a diode curve tracer. The upper two traces show the complete forward and reverse I-V characteristics, and the lower traces expand the fourth quadrant, which is the light-generated I-V characteristic. The cells are seen to be quite efficient in terms of the "fill factor" parameter. Figures 3 and 4 present the forward and reverse I-V characteristics, respectively, for the same two samples, measured point-by-point in the dark. If diode "a-factors", i.e., in $\exp(qV/akT)$, are calculated from the forward characteristics, it is found that at the higher voltages values of about 1.5 are usually obtained. This result indicates that previously reported values much greater than 2 were possibly in error because of bad contacts. As reported by Gill³, however, and as confirmed in this reported work, the "a-factor" is meaningless because of the temperature independence of the slope of the forward I-V characteristic.

The rather abrupt change in slope seen in Figure 3 for both samples has been observed frequently. Although it seems to occur more often with the B-face samples, it has also been found occasionally on an A-face sample. Most likely the breakpoint is the result of defects in the junction region which create additional energy states in the forbidden gap. Parker and Mead⁴ have recently



8-A(P)

8-B(P)

Fig. 2 - Dark and Light I-V Characteristics for an "A"-face and a "B"-face Sample, Both Dipped for 8 Hours

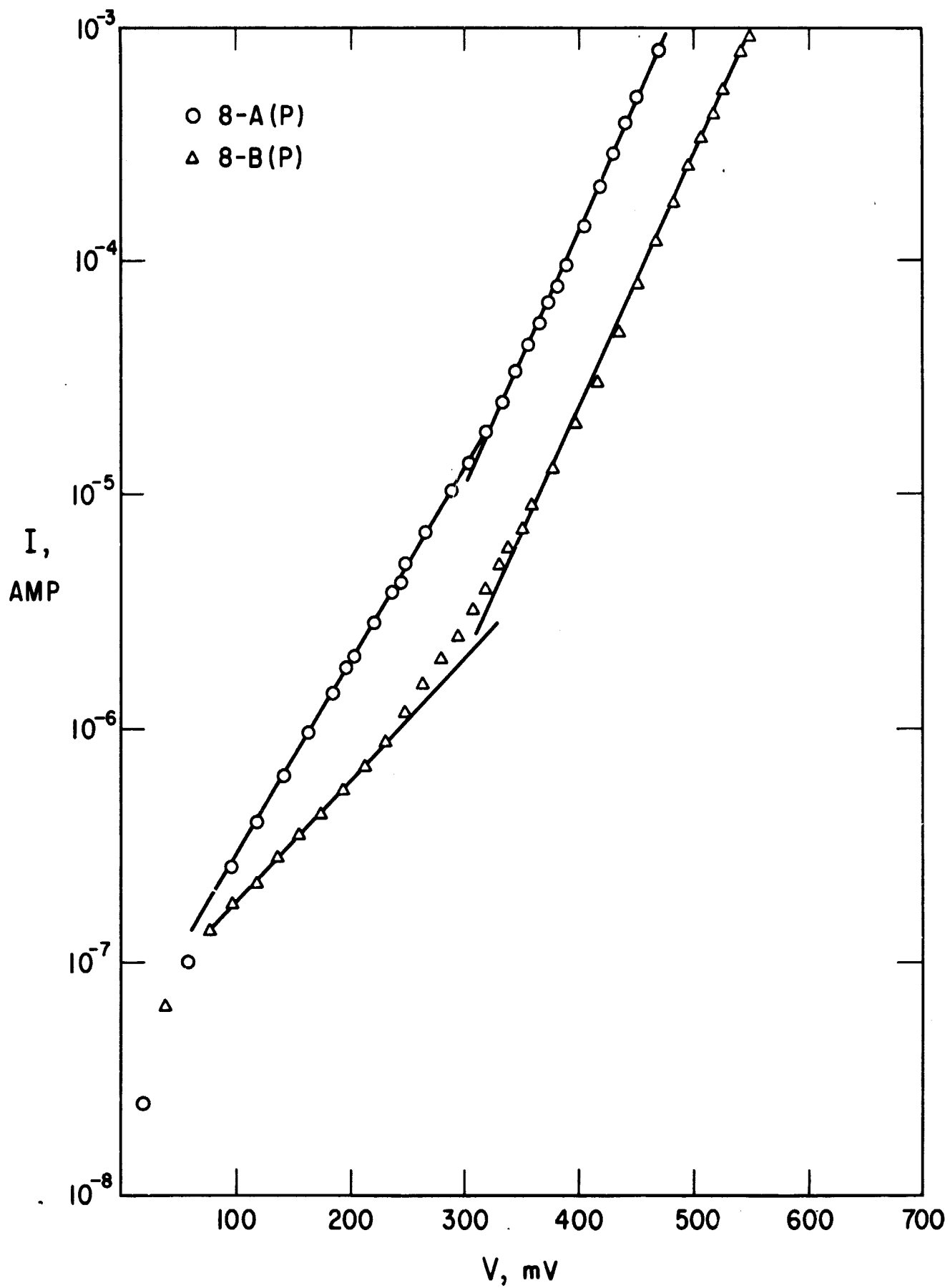


Fig. 3 - Forward I-V Characteristics in the Dark
 for 8-hour "A"- and "B"-face Samples

shown that such a break point can occur as the result of a two-stage tunneling process via an intermediate state caused by a defect.

The reverse characteristics in Figure 4 are fairly typical, with no saturation and an exponential variation of current with voltage over a range of several volts.

3. Capacitance-Voltage Curves

Figures 5 and 6 give C-V curves for two A-face and two B-face samples respectively. The Cu_2S thickness for each sample can be obtained from Table II. Both B-face samples, and the A-face sample with the thinner layer, follow very nearly the abrupt junction law ($n = 0.5$). The thick A-face layer sample has an entirely different behavior, however, with a much greater sensitivity of capacitance with respect to voltage than in the case of an abrupt junction. An intermediate thickness A-face sample gives a C-V curve with a slope intermediate between those shown in Figure 5. This effect has been observed sufficiently often to warrant its acceptance as a true characteristic of the A-face samples.

4. Spectral Response

Figures 7 and 8 are spectral response curves of short-circuit current and open-circuit voltage for an A-face and a B-face sample respectively. Both the I_{sc} and V_{oc} curves have been normalized to equal intensity. Both samples show good long-wavelength response out to 9000Å. The slight but noticeable structure around 11,500Å has not been explained, but does not seem to be an error in the intensity correction of the monochromator. Notice that V_{oc} for the B-face sample (Figure 8) drops off more sharply than I_{sc} at long wavelengths, whereas the difference between the two curves is not as great for the A-face sample (Figure 7). This feature is illustrated further in Figure 9, which gives the dependence of V_{oc} on the intensity of white light for the two samples of Figures 7 and 8. The relative intensity of unity is that

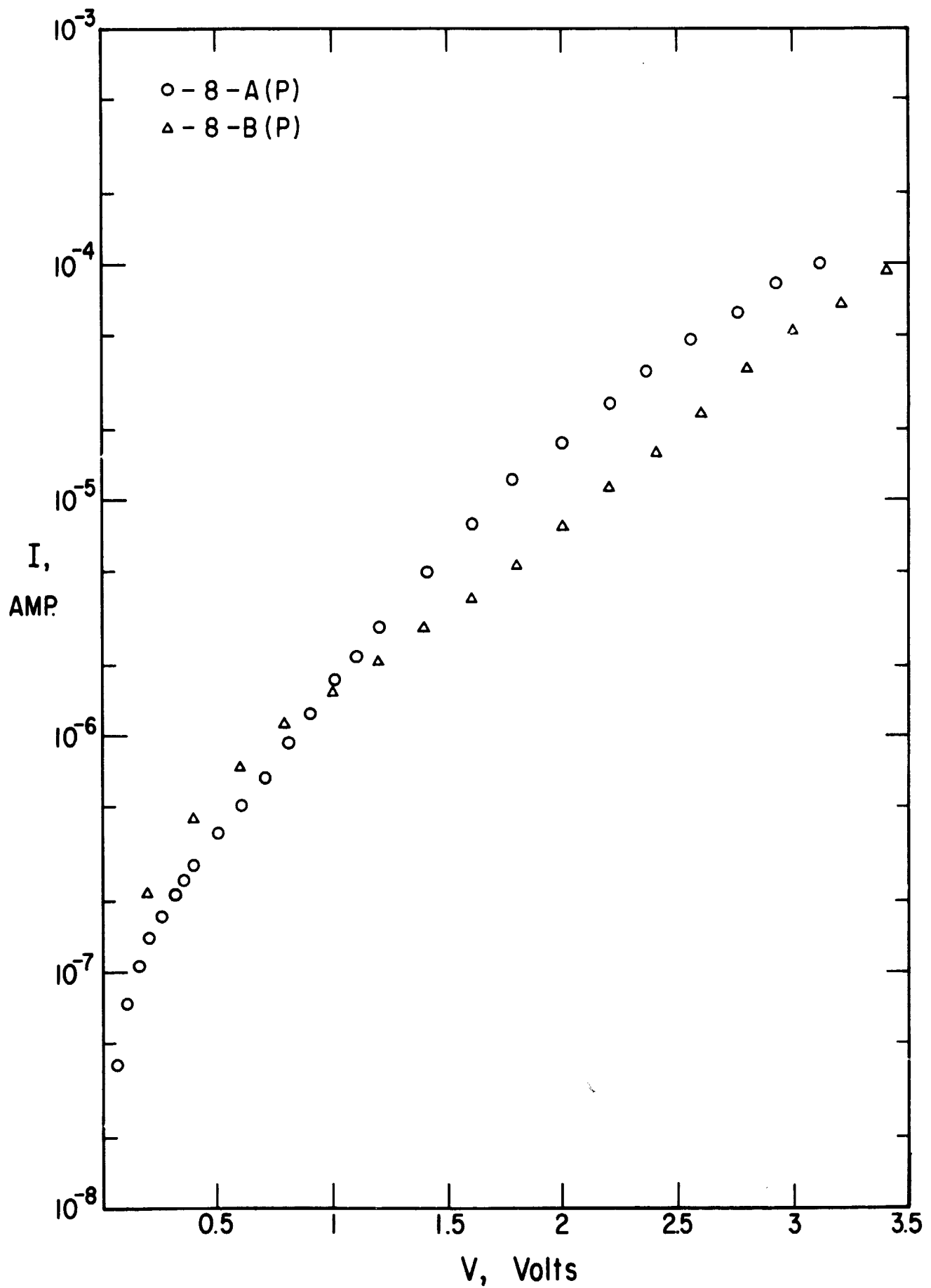


Fig. 4 - Reverse I-V Characteristics in the Dark
for 8-hour "A"- and "B"-face Samples

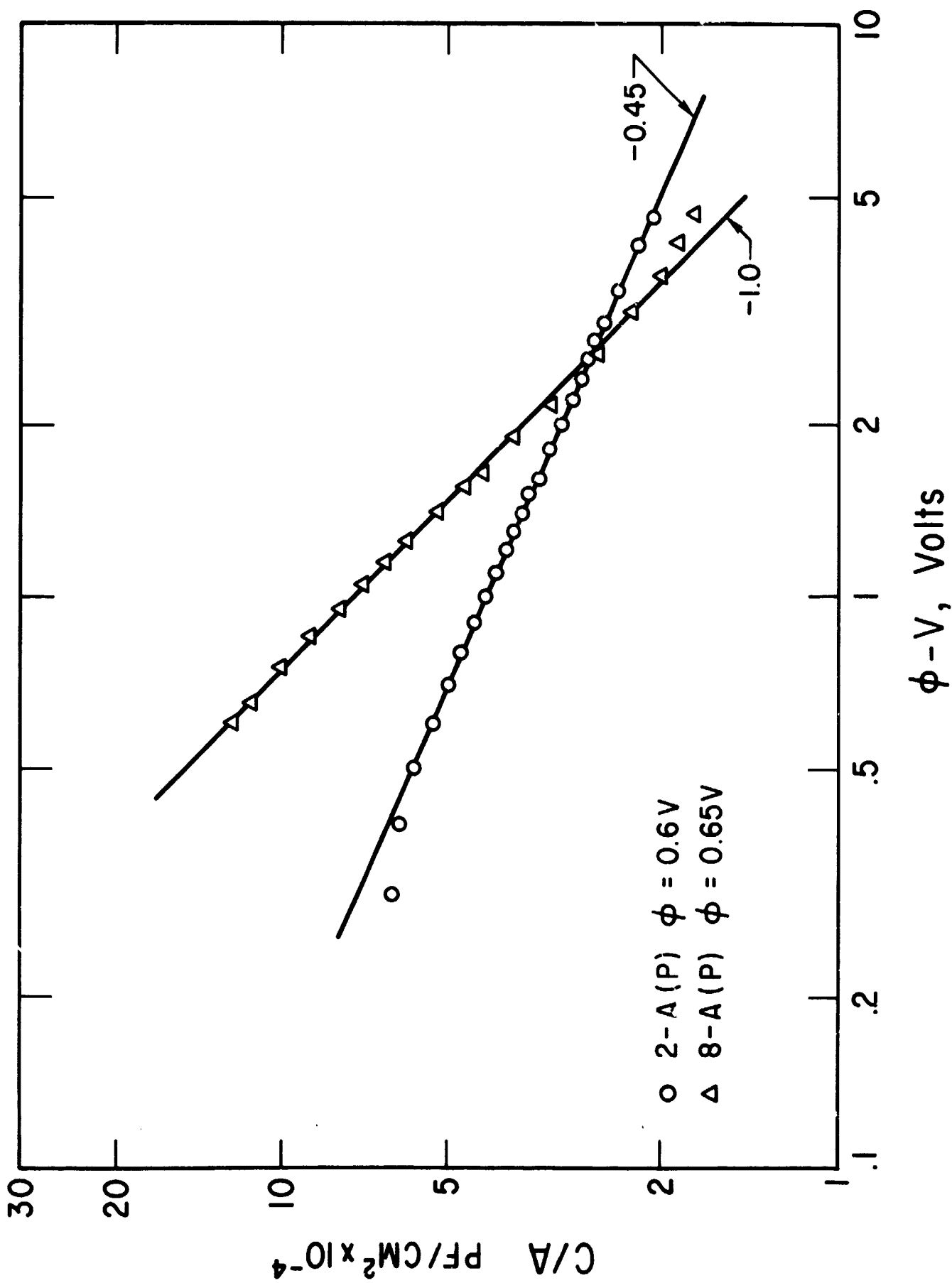


Fig. 5 - Capacitance-Voltage Curves for Two "A"-face Samples, Showing Effect of Increasing Cu₂S Thickness

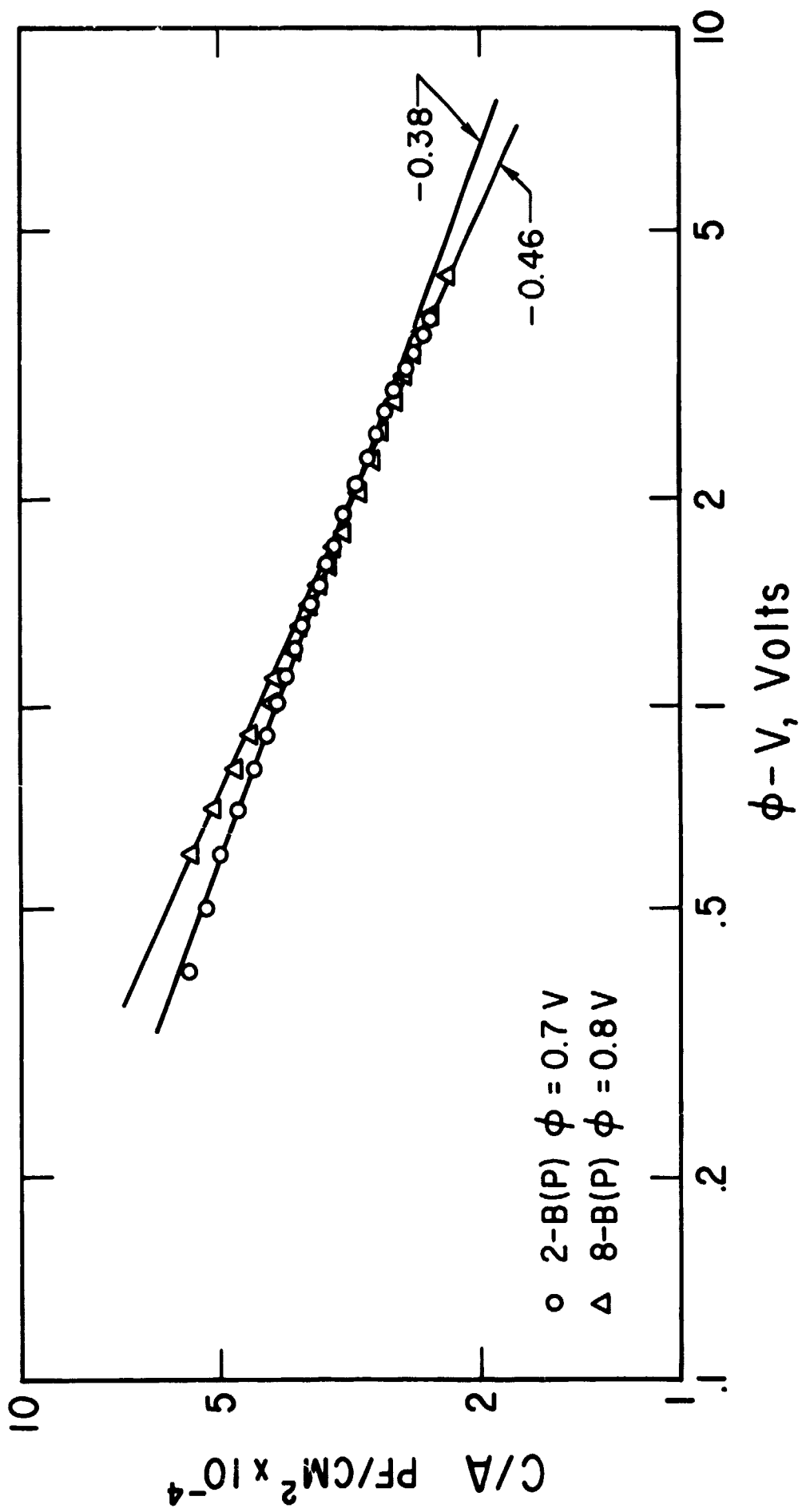


Fig. 6 - Capacitance-Voltage Curves for Two "B"-face Samples, Illustrating Weak Dependence on Cu₂S Thickness

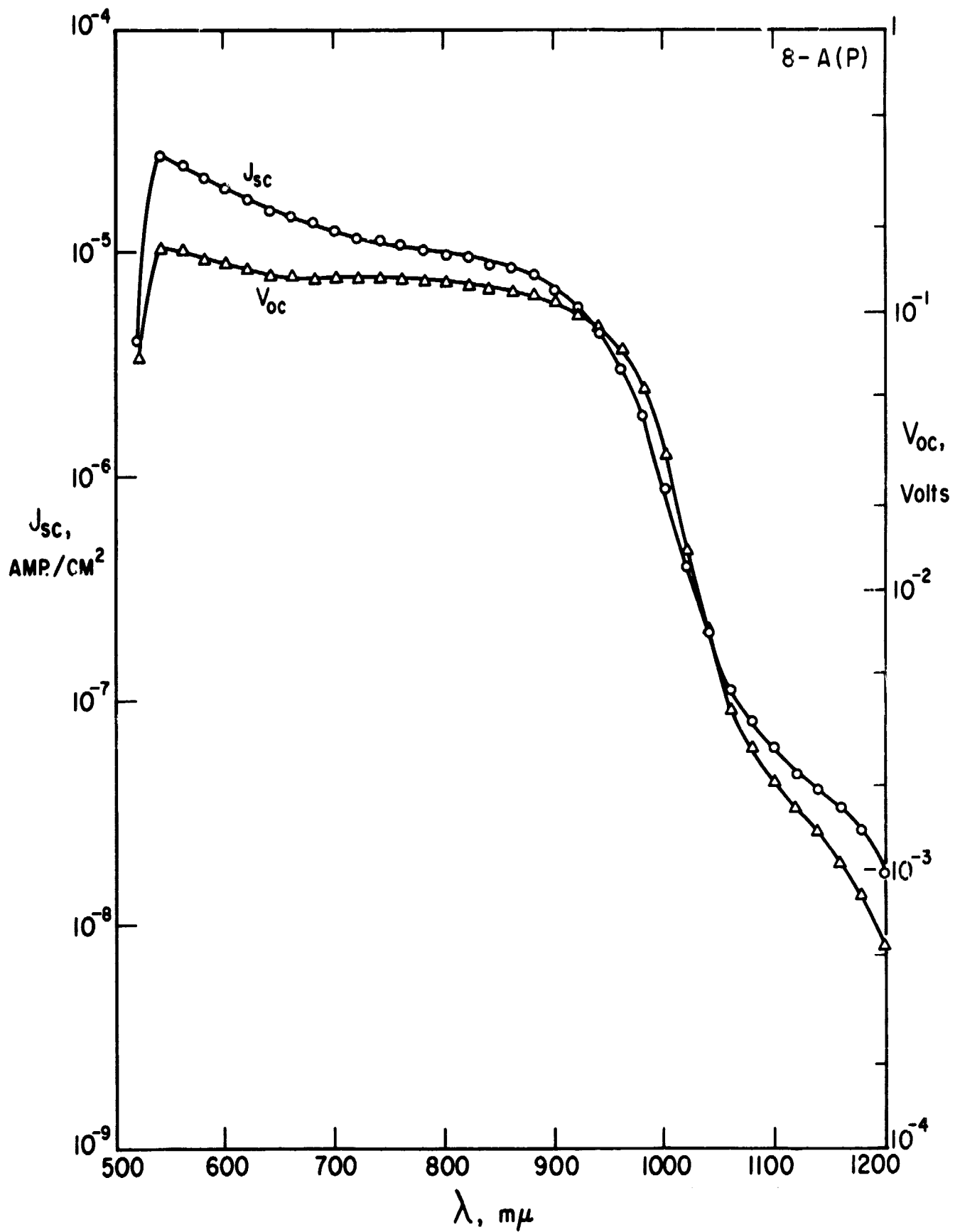


Fig. 7 - Spectral Response of Open-Circuit Voltage and Short-Circuit Current Density (Backwall) for 8-hour "A"-face Sample

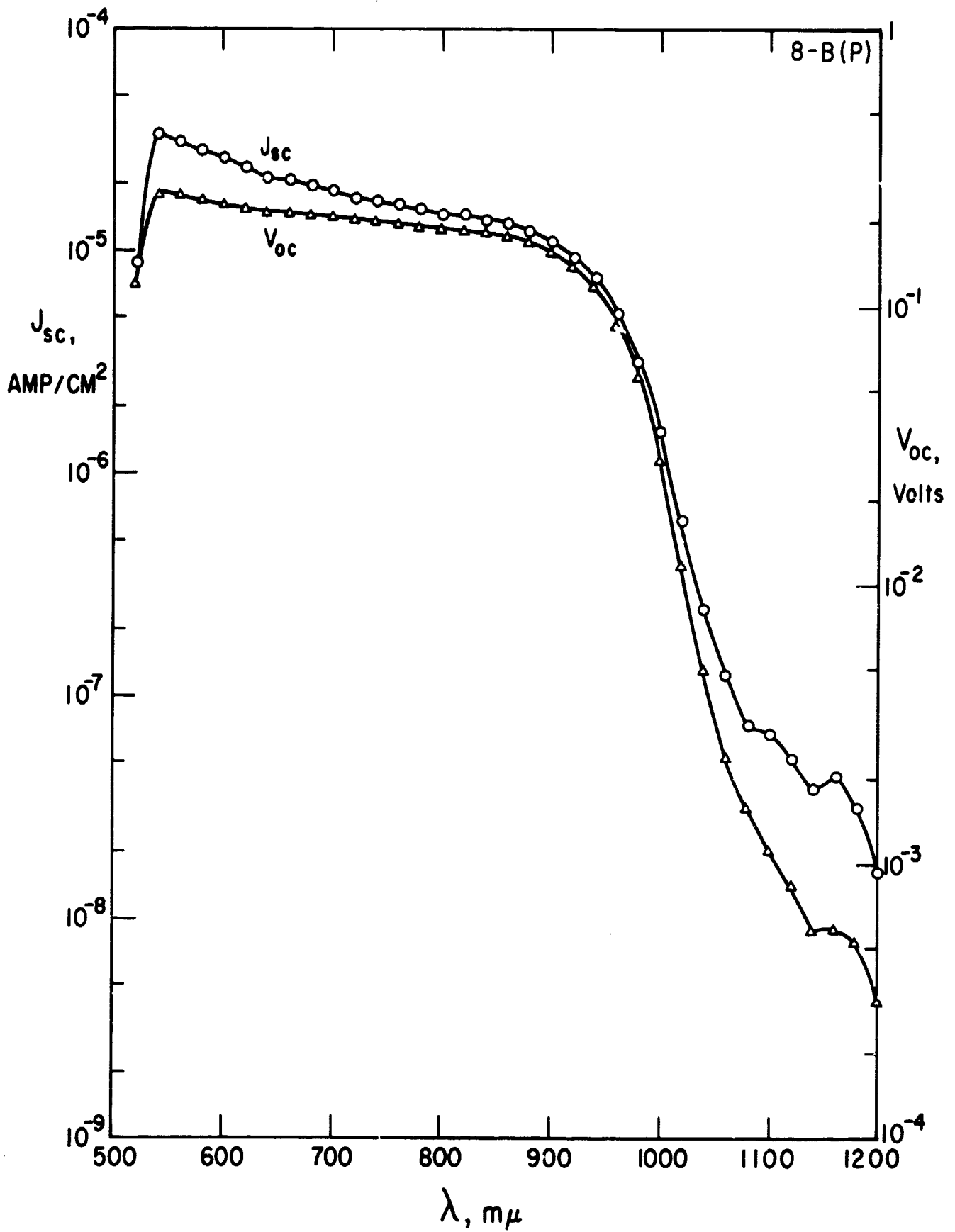


Fig. 8 - Spectral Response of Open-Circuit Voltage and Short-Circuit Current Density (Backwall) for 8-hour "B"-face Sample

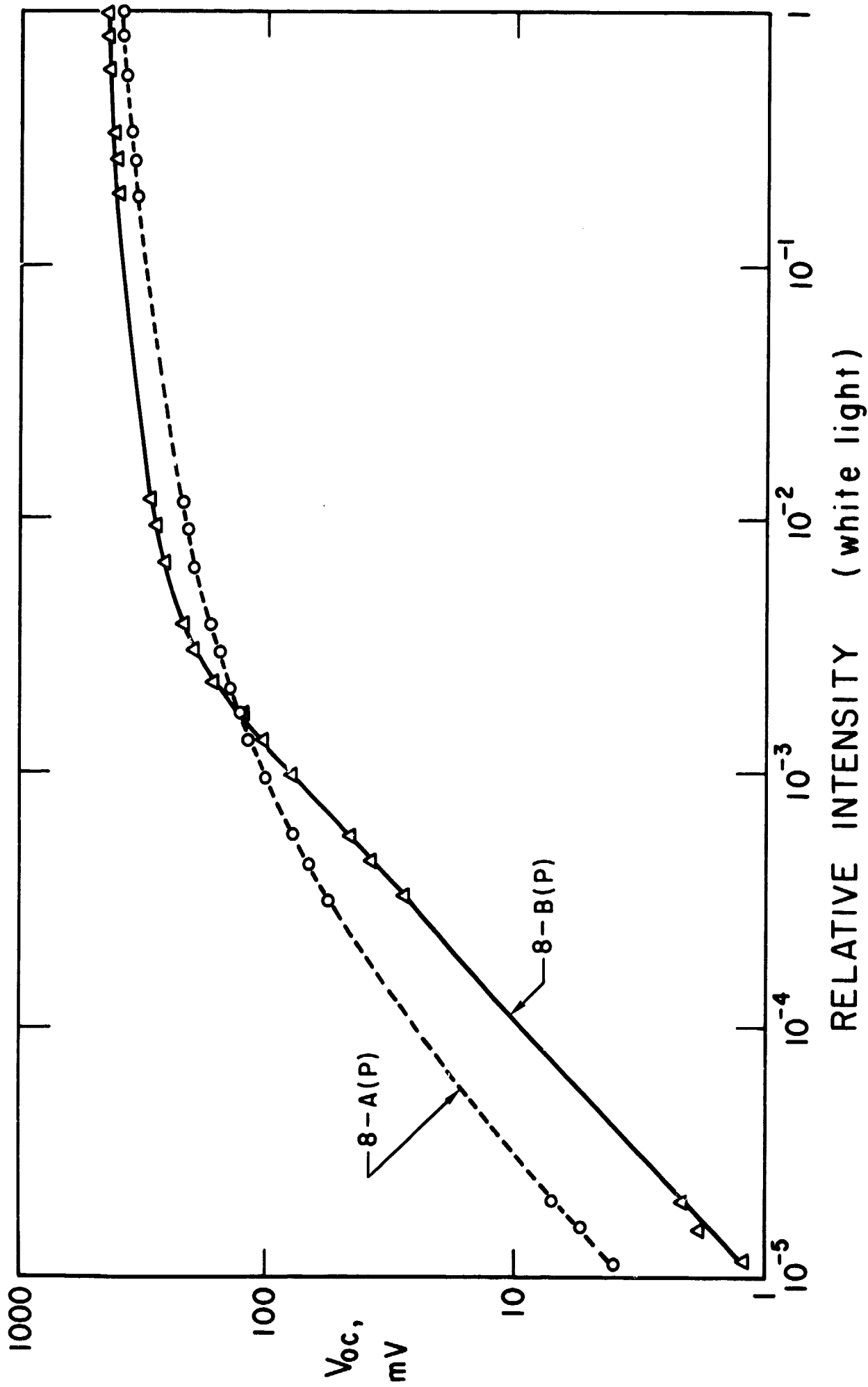


Fig. 9 - Dependence of Open-Circuit Voltage on Intensity of White Light for 8-hour "A"- and "B"-face Samples

intensity under which V_{oc} and I_{sc} were recorded in Table II, and which gave the light I-V curves of Figure 2. At high intensities, the B-face sample has a higher V_{oc} than the A-face sample, but the situation is reversed at a sufficiently low intensity. This behavior has also been observed with other corresponding pairs of A- and B-face samples and is apparently a characteristic difference of the two faces.

5. Time-Dependent Reverse Current in the Light

Figure 10 illustrates the characteristic transient behavior of all the cells measured at room temperature under simultaneous illumination (white light) and reverse bias. No difference in this behavior attributable to the A and B faces has been found. In Figure 10 the vertical axis is reverse current; V refers to the applied DC bias voltage; the time interval between successive events is of the order of 30 seconds. The transient occurs (a) with voltage on, when the light is switched on or off, and (b) with light on, when voltage is switched on only. The Figure is drawn for a sufficiently high reverse voltage that the dark current at that voltage, $I_D(V)$, is greater than the light current with no applied voltage, I_{sc} . It was found that the magnitude of the transient effect increases with increasing dark current. Thus for a very small reverse bias, less than one volt, almost no increase in the light current with time is seen. The presence of this effect rendered impossible the accurate measurement of AC photocurrent as a function of reverse DC bias, which yields a value for the diffusion length, a technique discussed by Logan and Chynoweth.⁵

6. Pulsed Forward I-V Characteristics

Figure 11 is a typical plot of forward current in the dark for two samples, measured with a pulse generator using a 1 percent duty cycle. The series resistance of the samples is about 5 ohms, and the intercept on the voltage axis gives the barrier voltage ϕ .

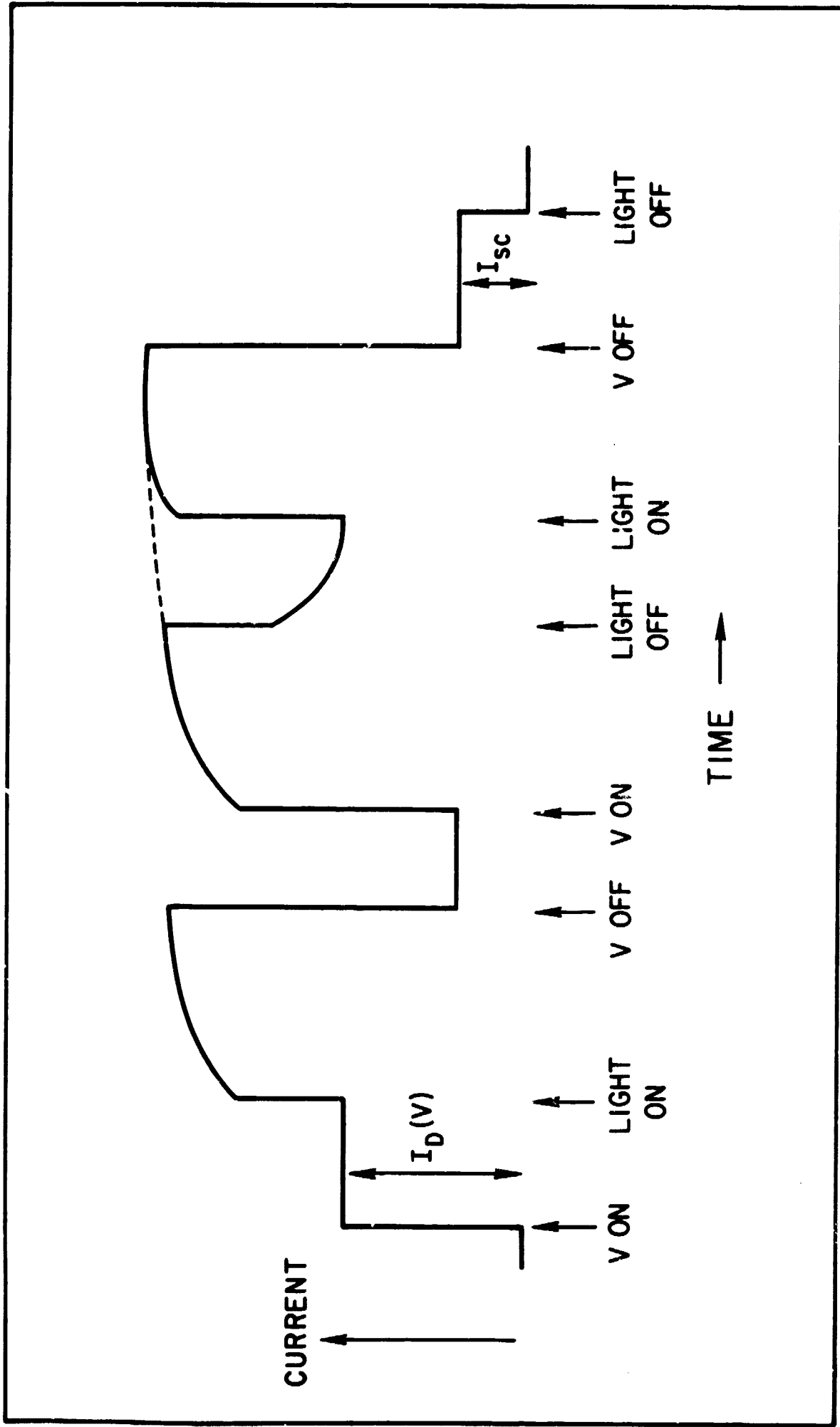


Fig. 10 - Schematic Illustration of Time-Dependent Reverse Current in White Light, Observed for All Samples at Room Temperature

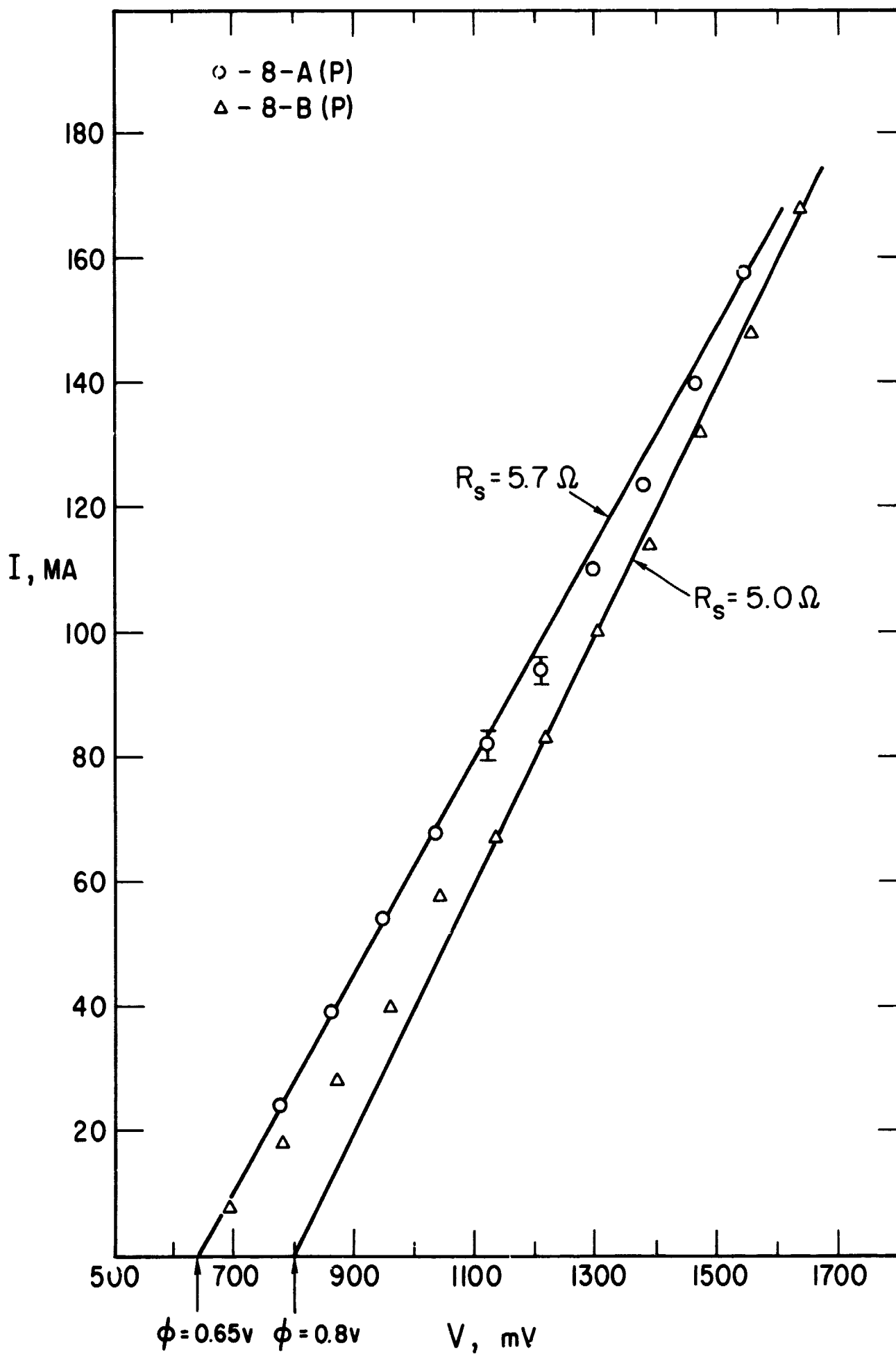


Fig. 11 - Pulsed Forward I-V Characteristics in the Dark for 8-hour "A"- and "B"-face Samples. Intercept on Voltage Axis Gives the Forward Barrier Voltage

B. Low-Temperature Measurements

Forward I-V characteristics from 298° to 150°K for an 8-hour B-face sample are shown in Figure 12. At the higher voltages, the slope of $\log I$ vs. V is independent of temperature. At lower voltages, the magnitude of the current becomes independent of temperature at sufficiently low temperatures, and in certain cases an increase in current at a fixed voltage has been noted with decreasing temperature. A plot of $\log I$ at constant V , vs. $1/T$, is curved, approaching a straight line only at the higher temperatures. Thus for the three highest curves of Figure 12, the current at 550 mv gives an apparent activation energy of 0.37 eV. These data suggest the possibility of a temperature-independent tunneling process at low temperatures, which becomes temperature-dependent at the higher temperatures.

Figure 13 shows the dependence of V_{oc} and I_{sc} on temperature for the same sample. The value of I_{sc} falls off approximately linearly with decreasing temperature, and the value of V_{oc} rises with decreasing temperature, exhibiting a maximum at about 160°K.

Figure 14 gives capacitance-voltage curves for an A-face and a B-face sample of comparable layer thicknesses (see Table II). At room temperature, the C-V curve for the A-face sample is steeper than that for the B-face sample, in accord with the previous discussion of Figures 5 and 6. As the temperature is decreased, with the sample kept in the dark, the C-V curves for both samples become steeper. The increase in capacitance at zero bias with decreasing temperature is somewhat surprising. For example, in the case of a p^+-n homojunction, the zero-bias capacitance varies as $(N_d/E_G)^{1/2}$, where N_d is the density of ionized donors on the n-side, and E_G is the band gap.⁶ Since for CdS the value of E_G increases with decreasing temperature,⁷ a corresponding decrease in capacitance would be predicted.

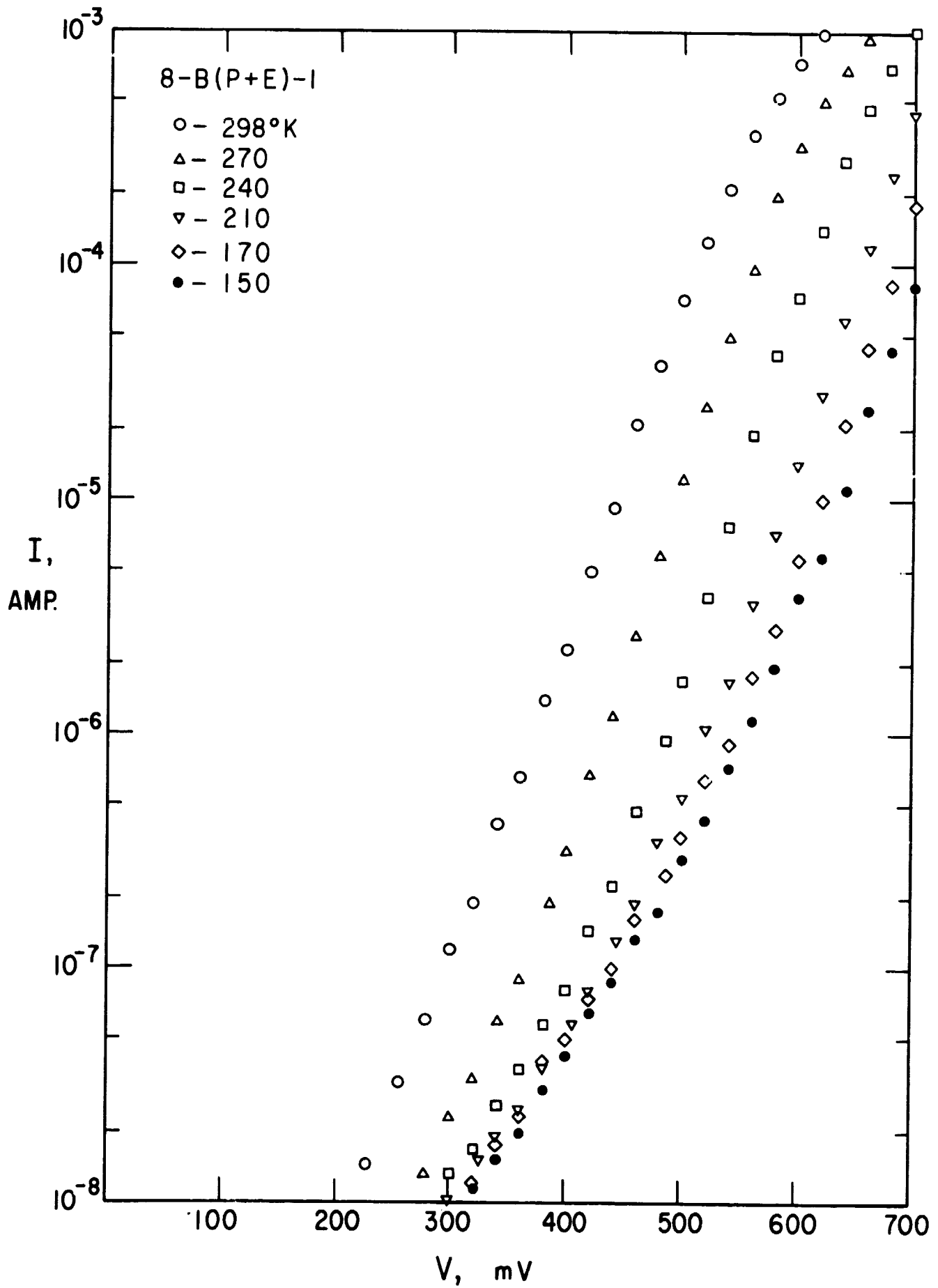


Fig. 12 - Temperature Dependence of Forward I-V Characteristic in the Dark for an 8-hour "B"-face Sample

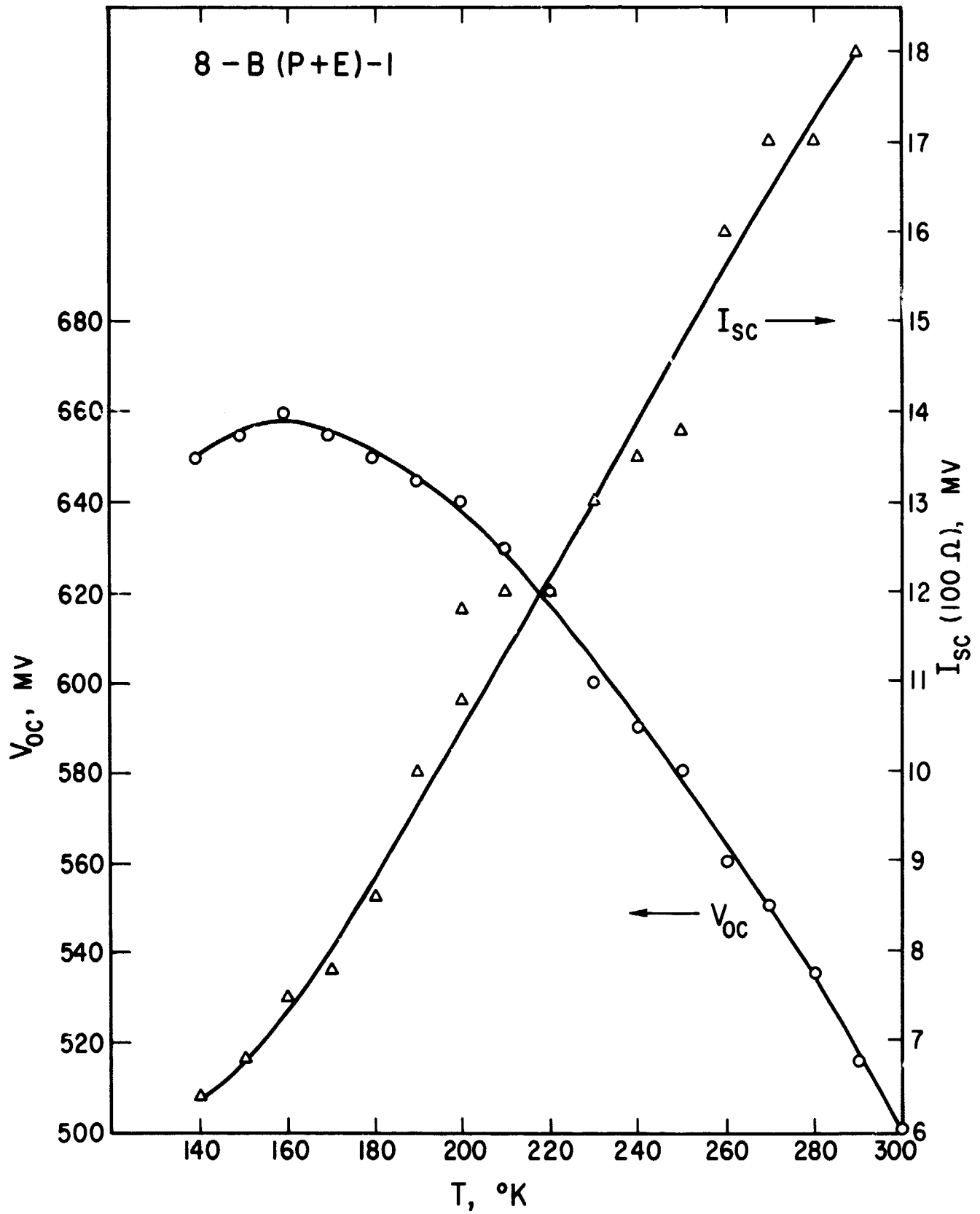


Fig. 13 - Open-Circuit Voltage and Short-Circuit Current as a Function of Temperature for an 8-hour "B"face Sample

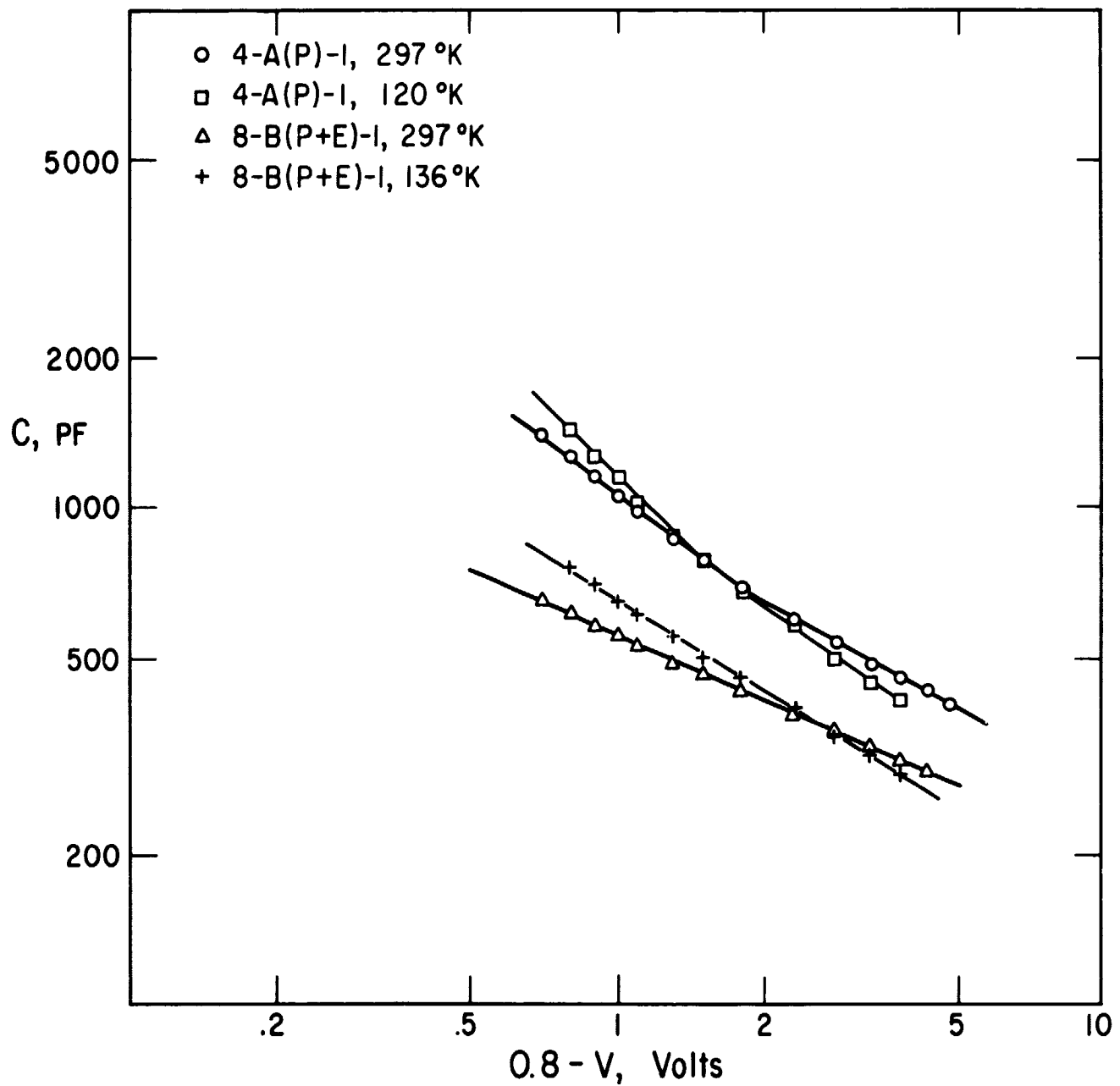


Fig. 14 - Capacitance-Voltage Curves for an "A"-face and a "B"-face Sample with Nearly the Same Cu_2S Thickness, Illustrating the Effect of Decreasing Temperature in the Dark. Value of $\phi = 0.8$ volt Assumed in Plotting the Data

Another phenomenon observed only recently is that of a persistent increment in capacitance after exposure to light at low temperatures. This is a definite indication of a trap-filling process which may be of fundamental importance to the operation of the cell. Such an effect can be used to obtain information about the nature of the states involved in the interface region and will be studied carefully for both A- and B-face samples.

IV. DISCUSSION

The data presented in this report indicate that photovoltaic cells with good spectral response characteristics can be produced without the heat treatment given the commercial thin-film cells. The spectral response of these single-crystal non-heat-treated cells, when compared with the spectral response of photoconductivity for a typical sample of "pure" 1 ohm-cm CdS measured by Gill³, shows that the response is not dominated by photoconductivity in the CdS. Rather, the good long-wavelength response of these cells is considered to be due to photoemission from the Cu₂S into the CdS, with carriers transported by tunneling through a discontinuity (spike) in the conduction band. In this view, the nature of the interface between the two crystalline phases is of great importance. The most efficient cells made during this work seem to be those in which the Cu₂S maintains an epitaxial relationship with the CdS substrate. The existence of an epitaxial relationship may be expected to influence the nature of any discontinuity in the conduction band.¹⁰

The C-V curves presented above demonstrate that, at least in the case of thin Cu₂S layers, the heterojunction may be considered to be abrupt. In the case of the thicker A-face samples, the steeper C-V plots could be interpreted in terms of a "retrograde" impurity profile as seen in the so-called "hyperabrupt" varactor diodes.¹¹ The probability of this interpretation is lessened, however, by the significant change in the slopes of the C-V curves with decreasing temperature. One property of the heterojunction which may

be expected to vary with both layer thickness and temperature is the stress at the heterojunction interface caused by the lattice mismatch between the Cu_2S and CdS. The existence of this stress, coupled with the highly insulating depletion layer in the CdS, leads to a consideration of the possibility of a significant piezoelectric effect in these cells. For a given mismatch strain caused by the discontinuity in crystal structure, the stress at the interface is a function of the elastic properties of the two materials, and their relative thickness. Thus the stress may be negligible for a very thin Cu_2S layer on a thick single crystal, but it may be appreciable in the case of a sufficiently thick Cu_2S layer on a single crystal, or in the case of the thin film cell in which the Cu_2S layer is again an appreciable fraction of the CdS film thickness. The possible role of the piezoelectric effect will be investigated by direct experiment.

V. CONCLUSIONS

Results to date of a systematic study of the effect of crystallographic orientation, layer thickness, and surface condition prior to dipping, may be summarized as follows:

1. The Cu_2S layer grows much more rapidly on the A-face than on the B-face. The thickness of the Cu_2S varies as t^n , with n slightly greater than unity for both faces.
2. V_{oc} in white light is consistently larger for B-face samples than for A-face samples. This relationship is reversed at very low light intensity. V_{oc} consistently decreases with increasing Cu_2S layer thickness.
3. J_{sc} decreases with increasing Cu_2S layer thickness for both A- and B-face samples. For thin layers the A-face samples have the larger J_{sc} .
4. The slope of the C-V curve for B-face samples is close to that for an abrupt junction and increases only slightly with increasing Cu_2S layer

thickness. For the A-face samples the slope increases rapidly with increasing layer thickness; interpretation of this effect could involve an anomalous in-diffusion of copper, or possibly a piezoelectric effect.

5. C-V curves in the dark increase in slope with decreasing temperature for both A- and B-face samples.
6. Slopes of the forward I-V characteristics in the dark are independent of temperature, confirming the presence of a tunneling process.
7. No significant differences between polished and etched samples were observed.
8. The time-dependent reverse current in the light at room temperature, and the low-temperature persistent photocapacitance effect suggest that interface states may play an important role in the operation of the junction.

REFERENCES

1. Grown by R. Feigelson, Center for Materials Research, Stanford University.
2. J. Singer and P.A.Faeth, Appl.Phys.Letters 11, 130 (1967)
3. W.D.Gill, PhD Thesis, Department of Materials Science, Stanford University,
June (1969)
4. G.H.Parker and C.A.Mead, Appl.Phys.Letters 14, 21 (1969)
5. R.A.Logan and A.G.Chynoweth, J.Appl.Phys. 33, 1649 (1962)
6. R.A.Smith, Semiconductors, Cambridge Univ. Press, p. 269 (1961)
7. R.H.Bube, Photoconductivity of Solids, John Wiley and Sons, New York, p. 237
(1960)
8. R.Williams, J.Appl.Phys. 37, 3411 (1966)
9. J.C.Carballes and J.Lebailly, Solid State Commun. 6, 167 (1968)
10. W.E.Howard and A.B.Fowler, J.Appl.Phys. 39, 1533 (1968)
11. R.L.Anderson and M.J.O'Rourke, IBM Journal, July (1960), p. 264